AIMS Materials Science, 6(3): 335–353.
DOI: 10.3934/matersci.2019.3.335
Received: 18 January 2019
Accepted: 18 April 2019
Published: 24 April 2019

http://www.aimspress.com/journal/Materials

Mini Review

Photocatalytic coatings via thermal spraying: a mini-review

Ionut Claudiu Roata, Catalin Croitoru*, Alexandru Pascu and Elena Manuela Stanciu

Department of Materials Engineering and Welding, Transilvania University of Brasov, 500036, Eroilor 29, Brasov, Romania

*** Correspondence:** Email: c.croitoru@unitbv.ro; Tel: +40748126598.

Abstract: Light-driven functional coatings present an enabling technology of major importance in the successful, effective, and efficient exploitation of materials for energy and environmental-related problems of modern-day society. Photocatalyst coatings are traditionally obtained through physical/chemical vapor deposition or sol-gel related techniques. All these processes have certain disadvantages such as high environmental footprint, low adhesion to the substrate, poor mechanical properties, which makes them less suitable for upscaling to pilot and industrial applications. Thermal spraying is nowadays a well-established technique that offers all the prerequisites for obtaining mechanically-resistant and highly efficient photocatalytic coatings, on practically all types of substrates (metals, polymers, ceramics) bearing a wide area of geometries. Even if thick coatings are usually obtained through the thermal spraying method, the inherent nanopatterning of the surface generated through impact and plastic deformation of the feedstock material with the substrate generates the high surface area required for an efficient photocatalysis process. This mini-review presents some of the most important research results in the application of thermal spraying for achieving photocatalytic coatings. All the major techniques related to thermal spraying are considered, starting with flame spraying and moving on to newly developed techniques, such as high velocity oxy-fuel spraying, plasma spraying and cold gas spraying.

Keywords: coatings; functional materials; photocatalysis; thermal spraying; flame spraying; HVOF spraying; plasma spraying; cold gas spraying; photodegradation

1. Introduction

Coatings represent complex structural interfaces, nowadays with practically unlimited possibilities of chemical speciation and structural architecture and with a wide application palette,

ranging in any proportion between purely decorative to functional, between nanoscale and macroscale level [1,2]. An insight into the application field of inorganic, organic and hybrid coatings obtained through complex criterial analysis of the information provided by the Web of Science platform (Clarivate Analytics, December 2018) has revealed that most of the research from the year 1975 up to date is focused on obtaining coatings with improved tribomechanical properties and corrosion resistance [3–5] (Figure 1a), followed closely by the catalytic applications (which include various aspects of synthesis, energy storage, photocatalysis, etc.) [6–8], biocidal (i.e., antibacterial and antibiotic character) [9,10], bio(medical), thermal, radiation, electromagnetic-insulative applications [11,12], and so forth.

For coatings of inorganic nature (which account for nearly 53% from the total, without considering composite-hybrid ones, based on the research data available from the Web of Science platform) several (electro)chemical or physical fabrication methods are available (Figure 1b) [13–18].

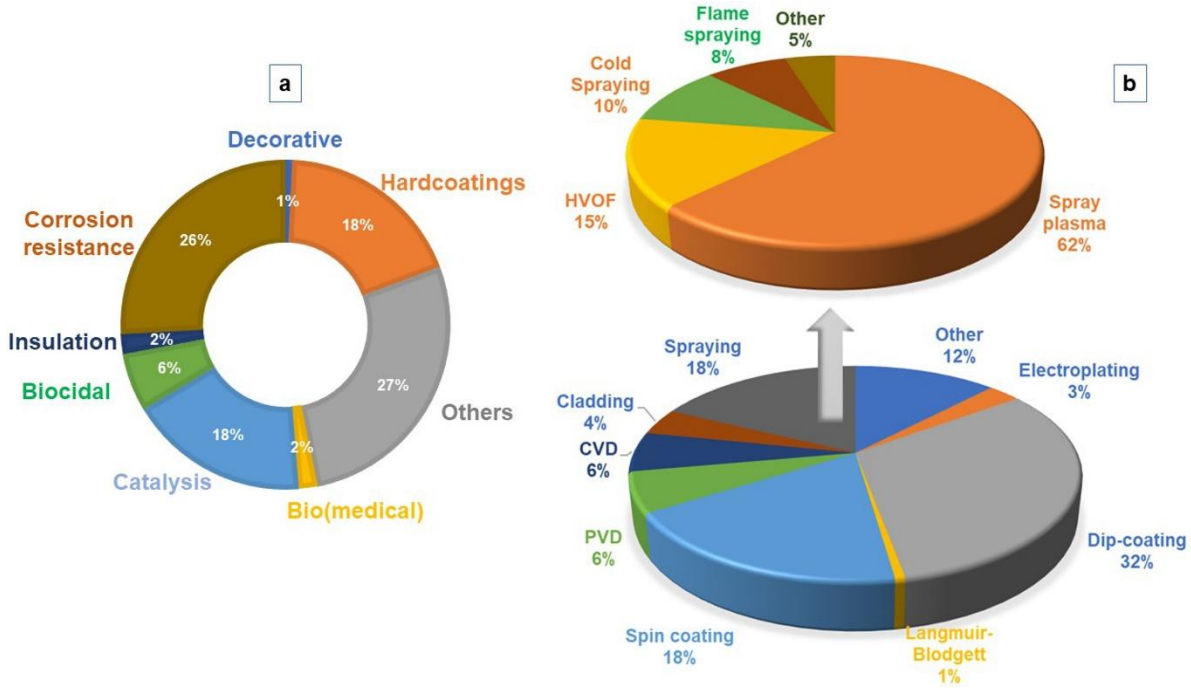

Figure 1. (a) coatings application domains and (b) frequently employed fabrication methods for inorganic coatings.

Among the physical fabrication methods, thermal spraying (with its technological variants) has been traditionally employed since the 1920's for achieving corrosion resistant hard coatings [19,20], reconditioning of worn metallic parts and tools [21], and more lately, to manufacture functional coating materials (thermal barriers [22,23], enhanced electrochemical response anodes [24], optically-active materials [25], semiconductors [26], biomaterials [27], solid fuel cells [28], and so forth).

All technological variants of this technique imply spraying a combustion flame- or plasma-heated feedstock material (which may be in the form of powder, wire, rod, liquid, etc.) onto a desired substrate (usually metal or ceramic) [29,30]. The melted or partly-melted feedstock (colloquially called "splat") is projected on the substrate with a high velocity, being deformed

(spread) onto the substrate surface on impact, generating a characteristic lamellar-layered coating upon its solidification [31]. Traditionally, coatings with thickness varying from 10 μm to a few mm can be obtained, but with the help of the high velocity oxy-fuel (HVOF) and plasma spraying techniques, the limit being lowered to 200–500 nm [32,33]. If the coatings are not nanometric, then nanopatterns can be exhibited on the surface in a highly reproducible manner [31,32].

This paper is focused on reviewing the current trends in photocatalytic coatings achievement through different thermal spraying techniques. Photocatalytic coatings represent the state-of-the-art in advanced oxidation processes for environmental and medical applications, in designing self-cleaning smart materials, converting raw materials into new useful products, in energy generating applications and so forth [30,34]. Traditionally, physical (PVD) and chemical (CVD) vapor deposition, along with the sol-gel (SG) process have been usually employed for most of the studies involving photocatalytic coatings achievement [35]. PVD and CVD have the advantage of obtaining photocatalytic coatings with tunable (and constant) chemical composition and thickness, avoiding the oxidation/chemical modification of the feedstock material during the deposition [30,36]. However, these are both energy-intensive and expensive processes, not currently upscalable to deposit coatings on large substrates. Sol-gel processes are instead more cost-effective, but also more time-consuming. Also, the chemical composition, morphology and the thickness of the SG coating is very difficult to be maintained, especially for large parts with complex geometry. Another issue that makes sol-gel processes less useful when considering upscaling to pilot or industrial-level applications is represented by the coatings low wear resistance, hardness and adhesion to the substrate. Also, as a trendline, there are comparatively fewer studies dealing with the obtaining of photocatalytic coatings on metal substrates (more relevant when considering the processes on a larger scale) with any of these techniques (PVD, CVD, SG), in comparison with ceramics, glass and organic substrates [37,38].

Even if thermal spraying can be currently considered as complete technique, it has all the requirements of being a successful candidate for photocatalytic coatings achievement: low equipment maintenance cost, lower environmental footprint (compared to CVD or PVD), versatility regarding the physical state and chemical composition of feedstock material (liquid precursors could be also sprayed, generating the photocatalytic coating on the substrate through the precursor decomposition; both metallic and high-refractory ceramic particles can be flame or HVOF-sprayed; even polymers can be successfully sprayed or employed as substrates for coatings with cold spraying technique), the possibility of application to large surfaces with complex geometry, the possibility of nanopatterning the surface, and so forth [38–41]. The disadvantages of thermal spraying reside mainly in unwanted oxidation of the feedstock material during spraying, which lowers the mechanical properties of the coatings and their adherence to the substrate which can be diminished by the adequate use of inert protection gases), and a more difficult control in the thermal sprayed coating thickness, which could be overcome by a careful controlling of the process operational parameters [42,43]. Another drawback could be constituted by higher deposition temperature (in flame spraying and plasma spraying technique) which affects the photocatalytic yield of the coating, due to allotrope/polymorph transformations of the material (e.g., in the case of TiO_2, high temperatures promote the anatase to rutile transformation) [44–46].

There are currently relatively few researches involved in photocatalytic coatings achievement through thermal spraying, this application being at present time under continuous development. New sub techniques, such as liquid precursor spraying or powder composite-aggregate spraying have

permitted the achievement of coatings with improved nanopatterned structure and photocatalytic response. Based on the data from the Clarivate Analytics Web of Science platform, it can be concluded that roughly 74% of the coatings applied in photocatalysis are TiO_2-based. Narrowing the domain of interest to photocatalytic coatings obtained by thermal spraying, TiO_2 coatings account for 84% of the total research. Based on criterial topic search algorithms, the majority of the thermally-sprayed photocatalyst coatings were deposited on glass and ceramic substrates.

The current state-of-the-art (mini-review) is focused on presenting several important developments and trends in the photocatalytic coatings developing through thermal spraying and could serve as a starting point for crystalizing new ideas in this broad research domain.

2. Methods of obtaining photocatalytic coatings

2.1. Flame spraying

Flame spraying represents the oldest thermal spraying technique. It implies the combustion of a fuel gas (typically acetylene) with oxygen to melt a feedstock material which is propelled on a substrate [47], as shown schematically in Figure 2.

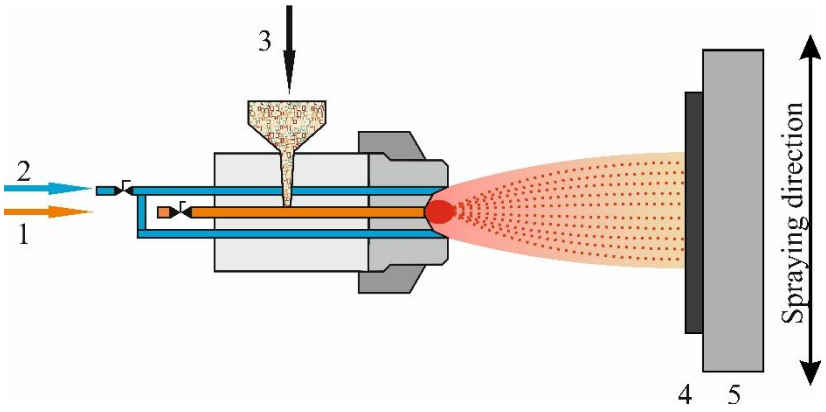

Figure 2. Schematic diagram of powder flame spraying. 1: fuel gas; 2: oxygen; 3: filler material (powder) and carrier gas; 4: spray deposit; 5: base material [48].

Flame spraying has been frequently used to generate high-quality wear- and corrosion-resistant coatings, or for reconditioning various metal parts, but to a lesser extent in the fabrication of photocatalytically-active coatings [30]. Flame spraying technique generates the second highest processing temperatures (typically in the range of 2500–3400 °C) after plasma spraying [49]. With this thermal spraying technique, the oxidation of feedstock is to a considerable extent almost inevitable [50]. The so called “time of flight”, i.e., the time required for the feedstock to travel from the thermal spray nozzle to the substrate is a crucial parameter in the flame spraying technique. It needs to be carefully chosen, by tuning the distance between spraying gun and substrate material [30,50,51].

Usually the feedstock is in powder form (metal or ceramic), but suspensions have also been recently used with high velocity suspension flame spraying (HVSFS) variant. In the HVSFS technique, the conventional gas-fueled torch is modified in order to process liquid feedstock.

Moreover, with this technique, organic solvents (i.e., aliphatic alcohols) injected into the HVOF flame undergo an exothermic combustion reaction, increasing the heat input conferred to the particles. The resulting combustion gasses add a supplementary drag to the particles exiting the spraying gun determining a more efficient packing of the sprayed material, i.e., higher density of the coating [52,53].

Various processes have been developed to obtain micro and nanoparticulate photocatalysts, employing the use of metal-organic precursors, or custom liquid fuels (aliphatic alcohols) instead of gaseous hydrocarbons [54,55] but photocatalytic coatings obtained by flame spraying have been relatively sparingly studied.

Kavitha et al. have obtained titania films on silica substrates by flame spraying of a stabilized hydrous titanium oxide ($Ti(OH)_4$) sol. The band gap of obtained films ranged from 3.11 to 3.16 eV. Remazol brilliant blue dye was successfully degraded by the films under UV light irradiation [56]. Similarly, Yang et al. have obtained rutile-rich nanostructured coatings starting from butyl titanate. They have proposed a mechanism for the nucleation of the rutile phase, starting from the surface of the initial anatase, resulting in a hybrid surface with a rutile outer layer and an anatase core [57].

Liquid flame spraying could be considered a simple method to obtain doped photocatalyst coatings. Yang et al. have obtained Ag^+-doped-nanostructured TiO_2 photocatalytic coatings by using this approach. The phase structure of coatings was not significantly influenced by the silver ion doping, but the photocatalytic activity of doped coatings was higher than that of the reference TiO_2 coating, regardless of the dopant concentration [58]. In another study, the same group obtained Cu^{2+}-doped TiO_2 coatings. The enhancement of photocatalytic activity when adding the dopant could be attributed to the adsorption ability of oxygen and other reactants on the surface of the TiO_2 coatings [59].

Ctibor et al. have used a commercially-available anatase-rich TiO_2 powder, a pre-reduced TiO_x powder and a powder agglomerated from nanometric particles as feedstock for obtaining porous coatings photocatalytically-active in the UV domain, using acetone as degradation model compound. They have found that through flame spraying, the anatase phase is preserved in a higher amount in comparison with plasma spraying [60].

Huang et al. have obtained nanocomposite titania-hydroxyapatite-reduced graphene oxide coatings by liquid flame spray deposition. An aqueous suspension containing submicron particles of the components has been used as feedstock for spraying on stainless steel. Two variants of nanopatterned coatings have been obtained: with thickness of 120–150 μm and 20–30 μm. A maximum BET surface area of 0.8 m^2/g was responsible for a good photocatalytic response regarding the UV degradation of methylene blue dye [61].

Roata et al. have used a different approach in designing thick photocatalytically-active coatings on copper substrates. They have employed an aluminum bronze powder (containing also small amounts of iron) as feedstock material and a conventional flame spraying torch. The photocatalytic response of the coatings was generated by the copper and iron oxides developed during the spraying of the metal powder. By varying the distance between the flame spraying torch and the substrate between 150 and 200 mm, coatings with different oxide contents and photocatalytic activities could be obtained. Moreover, the attained oxides present a nanopatterned texture, and the metal (mainly Al) acts as charge carrier separation means, contributing to the overall efficiency of the coatings for the UV-driven methylene blue degradation [30].

Navidpour et al. have obtained hematite coatings through plasma and flame spraying techniques

on 316 stainless steel plates, starting from pure hematite as the initial feedstock powder. The average size of the particles was around 5 μm. The thermal spraying distance greatly influences the hematite/magnetite ratio. In this respect, the weight percent of the hematite was decreased by increasing the distance of the spraying torch from the substrate, consequently with the visible light-mediated photodegradation efficiency against methylene blue aqueous solutions [62]. Flame-sprayed coatings were more photocatalytically efficient than plasma-sprayed coatings, due to their higher active surface and α-Fe_2O_3 content.

2.2. HVOF thermal spraying

In the high velocity oxy-fuel (HVOF) variant of thermal spraying, the feedstock material is accelerated at supersonic velocity through a converging or converging/diverging nozzle by means of the rapidly expanding gases evolved in the chemical reactions between hydrogen and oxygen, or gaseous hydrocarbons and oxygen (Figure 3) [63,64]. This allows for lower temperatures (hence lower oxidation degrees and chemical degradation of the coated material) and better mechanical bonding of the coating with the substrate than in the case of conventional thermal spraying [65].

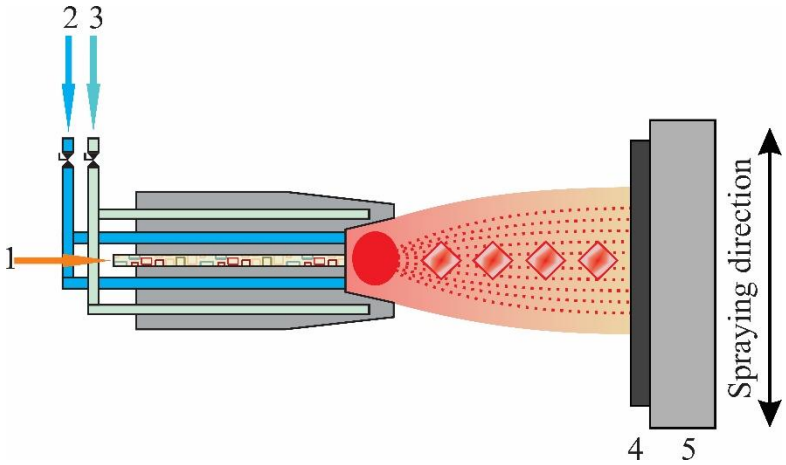

Figure 3. Principle of high velocity and fuel gas flame spraying. 1: filler material (powder) and carrier gas; 2: oxygen or air fuel; 3: cooling system (water or air); 4: spray deposit; 5: base material [48].

Up to date, there are only a few studies, regarding the application of HVOF to obtain TiO_2 thick and hydrophilic coatings in order to remove organic pollutants in gaseous phase. Titania represents probably one of the most widely employed photocatalysts [66], due to the ability to function as a photocatalyst under UV irradiation and to easily tunable photocatalytic response through doping or mixing with species that facilitate charge carriers separation. High anatase/rutile ratios can be generally obtained through HVOF, with increased surface areas which is beneficial for photocatalysis [67,68].

Toma et al. have obtained 5–20 μm thick photocatalytic TiO_2 coatings through HVOF spraying for photodegradation of NO and NO_x nitrogen oxides [69]. The feedstock material comprised of anatase-rich and anatase-10 wt% Al micro-sized powders, or micro-agglomerated TiO_2 (92% anatase) powders. It has been observed that after the HVOF process, anatase converts into the rutile

polymorph, which presents a lower photocatalytic efficiency than anatase (the anatase content was only ~12% after spraying). The Al provides a more efficient charge carrier separation during UV-light irradiation, leading to improved efficiencies. The values of the conversion ratio ranged between 30 and 32% for NO and 16–18% for NO_x [70]. In another study, Toma et al. have obtained HVOF-sprayed coatings starting from aqueous suspensions containing 40 wt% rutile and anatase phases, using ethylene as fuel gas. The parameters of spraying process were chosen to obtain mechanically stable coatings and to preserve a high content of the initial crystalline phases of the powders [71].

Colmenares-Angulo et al. have performed a comparison between the photocatalytic activities of HVOF and plasma-sprayed TiO_2 coatings. Partially reduced oxidic species were registered in all coatings, such as Ti_8O_{15}, which are detrimental for photocatalysis applications. As-prepared samples showed limited photocatalytic activity towards methylene blue degradation, but with the HVOF-generated coating being more efficient than the plasma-sprayed one. In contrast, post-deposition oxidation of the samples in air resulted in significantly improved catalytic performance of the coatings, due to the increase of the anatase content [72]. Detailed structural studies performed by Yang et al. have indicated that the rutile phase in plasma-sprayed TiO_2 presents a more significant preferential orientation along the (101) atomic plane than the same material deposited through HVOF, due to the tensile stresses concentrated in the individual splats. The (101) diffraction planes may change their orientations parallel to the coating surface under tensile stress at high temperature during splat cooling. This preferential orientation has a negative influence on the efficiency of the photocatalysis process [73,74].

The comparative study on the microstructure and photocatalytic properties of titanium dioxide coatings obtained by different thermal spray methods: atmospheric plasma spraying, suspension plasma spraying, and HVOF using agglomerated and nonagglomerated TiO_2 nanopowders as feedstock materials led by Toma et al. has indicated that the coatings elaborated by suspension plasma spraying presented a specific structure that depended on the nature of the solvent used in the preparation of the suspensions. The coatings obtained starting from aqueous suspensions were able to preserve a higher ratio of anatase than in the case of alcoholic feedstock powder suspensions, therefore showing remarkable photocatalytic efficiency that in some conditions was higher than that of the corresponding anatase powder [75].

Similarly, Ctibor et al. obtained rutile-rich TiO_2 coatings through HVOF, with band gap energies ranging from 2.17 to 3.15 eV, efficient for UV photodegradation of acetone [76]. Different researchers have obtained TiO_2 coatings with higher anatase contents (35 to 55%) through modifying the geometry of the thermal spray nozzle, allowing lower temperatures, below that corresponding to the anatase-rutile polymorph transition at ~600 ℃ [77] Bozorgtabar et al. have obtained a coating containing 80% anatase by volume at 120 mL/min low fuel flow rates. The results show that the as-sprayed TiO_2 HVOF coatings were highly photocatalytically reactive for the degradation of ethanol [78].

Studies led by Pala [79] have indicated that nanopatterned and anatase-rich (20.45–69.14%) coatings can be obtained by suspension high velocity oxy-fuel spraying approach (principle scheme shown in Figure 4), with potential photocatalytic and/or sonophotocatalytic applications. In their study they have used anatase nanoparticles (with diameters between 50 and 180 nm) 20 wt% suspensions in water, which they have directly injected into the center of the HVOF combustion chamber.

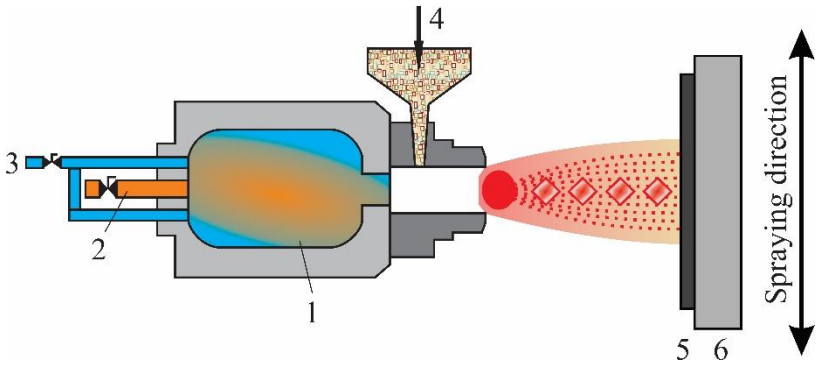

Figure 4. Principle of high velocity liquid/suspension fuel flame spraying. 1: combustion chamber; 2: liquid fuel; 3: oxygen/air; 4: suspension/solution and carrier gas; 5: deposit/coating; 6: base material [48].

Higher heat powers lead to the achievement of surfaces with higher roughness as well as to the presence of micro- and nanopatterned formations that could be beneficial for catalytic applications.

2.3. Plasma spraying

This variant of thermal spraying uses DC- or RF-generated plasma as a spraying heat source. Owing to high temperatures of the plasma, a wide range of refractory ceramics and alloys could be successfully sprayed at velocities of 200–300 m/s. With this thermal spraying technique, powders as well as liquid precursors and particle suspensions could be used as feedstock materials (Figure 5).

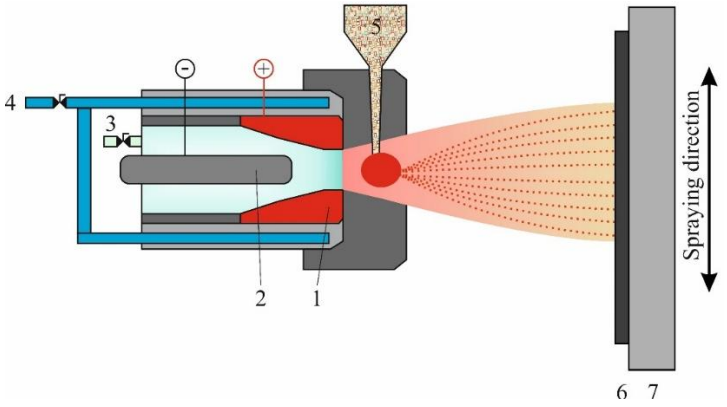

Figure 5. Schematic diagram of air plasma jet spraying unit. 1: anode; 2: cathode (electrode); 3: plasma gas; 4: cooling system; 5: filler material (powder) and carrier gas; 6: spray deposit; 7: base material [48].

As a general trendline, plasma spray ceramic coatings present an inherent connected-pores structure, which is beneficial for photocatalytic activity. Considering that usually splat size of micrometer scale into account, the surface area is not so high as other type of coatings (e.g., obtained by flame spraying) [80–82].

In some cases where the high temperature of the plasma spray process promotes undesirable

changes in the coating structure, it has been found that spraying with suspensions and liquid precursors is more benefic in obtaining a higher photocatalytic yield of the coating [83]. During suspension/precursor droplets spraying, the liquid dispersing media/solvent is evaporated, resulting submicron-agglomerated particles, which are melted and accelerated to the substrate.

Dosta et al. have obtained highly stable TiO_2 coatings with a wide range of structural characteristics for their application as photoanodes, starting from conventional rutile and anatase powder aqueous suspensions as spraying materials. The solar-irradiated photoelectrocatalytic performance for degrading Acid Orange 7 dye was 70% [84]. An aqueous suspension of Degussa P25 TiO_2 has been employed by Vu et al. to obtain UV-photocatalytic coatings by plasma spraying. They have found that the heating of the Degussa Powder at temperatures of 800 ℃ generates pure rutile of about 200 nm crystallite size in the coating [85].

Solonenko et al. obtained titania coatings on stainless steel by plasma spraying of an ethanolic solution of titanium tetra iso-butoxide precursor, which decomposes thermally into TiO_2. The novelty of the study consisted in using a specially-designed cascade plasma torch operating on argon-helium mixture which owed for an increased anatase content in the sprayed coatings. Good mineralization of the model dye compound has been achieved after 6 hours of UV-light irradiation [86]. Regarding TiO_2 coatings, it has been found that a minimum 15–20% anatase content is required for efficient photocatalysis. Another issue related to spraying TiO_2 is that fully-oxidized coatings are rarely obtained, with several other undesired phases being developed, such as Ti_2O_3 and TiO. A post-deposition heat treatment (650 ℃, 48 hours) ensures the complete oxidation of titanium to Ti^{IV+}, subsequent with the anatase to rutile transformation [87].

Ctibor et al. have proven that the initial morphology of the feedstock powder has a low influence on the microstructure of the plasma-sprayed coatings of titanium dioxide. This influence is more significant when discussing the photochemical response and respectively phase composition and crystallite size [76,88]. Since UV light generating is energy-intensive and it accounts for only ~5% of the solar spectrum, intensive research has been focused on obtaining photocatalytic coatings that are able to harvest light in the visible domain of electromagnetic radiation [89]. In this respect, suspension plasma spraying has been applied by Zai et al. for obtaining composite Ti_2O_3–TiO_2 coatings with reduced band gap (2.71 eV). The sprayed aqueous suspension contained Degussa P25 TiO_2 nanoparticles and surfactant polymers. The coatings present fine nanometric and submicrometric grains, have a gray color, thus being more efficient in light absorption. The coatings present an efficiency of 89% for degradation of aqueous methylene blue dye [90].

In another study, Ctibor et al. have used gas-stabilized (GSP) and water-stabilized (WSP) plasma guns to obtain TiO_2–Fe_2O_3 composite powders by atmospheric plasma spraying (APS). The novelty was to use a phase-controlling Na_2SiO_3 additive suitable for feeding into the plasma jet. The GSP coating has the best photocatalytic activity under both UV and VIS light irradiation. The coatings produced with the Na_2SiO_3 additive were dominatingly amorphous and more active in the UV domain [91].

Through the solution precursor plasma-spray route (SPPS), ZnO films with nanostructured surface morphologies have been obtained by Yu et al. [92,93]. Zinc acetate has been chosen as precursor, being dissolved in a water-ethanol mixture at concentrations ranging from 0.2 to 0.4 mol/L. Needle and bud-like nanopatterns were formed on the surface of the coatings, which were responsible for degradation of Orange II dye in under 100 minutes, under UV irradiation conditions. The assemblies presented bandgap values of 3.02 eV. Zinc oxide coatings could be obtained also

through traditional plasma-spray routes. For example, Navidpour et al. have obtained coatings with specific surface areas of 25–45 m^2/g starting from ZnO powder with an average diameter of 2 μm, with moderate efficiency in photodegrading methylene blue dye [94]. Through the same technique, Chen et al. have obtained highly porous titania surfaces using titanium isopropoxide in aqueous phase as precursor. The amount of anatase and rutile phases in the as-sprayed coatings can be adjusted by simply changing the plasma power. With the increase of plasma power, the coating anatase content decreases and the rutile content increases [95].

Coatings with a wide palette of chemical compositions can be obtained with plasma spraying technique. Doping the main photocatalytic-active feedstock material is facile, by mixing the appropriate amount of dopant with the liquid precursor, or through mixing powders with different chemistry in the desired ratios. For example, composite coatings have been obtained by Zeng et al. by powder plasma spraying of TiO_2 and $ZnFe_2O_4$ powders under various mixing ratios. The maximum methylene blue decomposition efficiency was ~75% under UV (365 nm) irradiation [96,97]. Platinum-doped TiO_2 coatings have been obtained by powder plasma spraying. The obtained coatings present ~70% photo-efficiency under light irradiation combined with a 15 V potential bias [98].

Composite TiO_2–Fe_3O_4 coatings have been obtained by co-spraying powder mixtures with various compositions, namely TiO_2–5 wt% Fe_3O_4, TiO_2–10 wt% Fe_3O_4, TiO_2–12.7 wt% Fe_3O_4, TiO_2–22.5 wt% Fe_3O_4 and TiO_2–32.6 wt% Fe_3O_4 powders. The coatings were able to completely degrade gaseous acetaldehyde in about 120 min [99].

Dom et al. have obtained ~25 μm-thick photocatalytic composite coatings starting from aqueous and organic (ethylene glycol) precursor solutions Zn^{2+} and Fe^{2+}, complexed with citric acid. Preparation of a stable precursor by metal–citrate complexation has been found to inhibit the oxidation of individual metallic species during film deposition. The chemistry of the coatings was mainly $ZnFe_2O_4$. This phase exhibited a band gap of 1.9 eV. The highly porous nature of the film favored its photocatalytic performance as indicated by methylene blue discoloration under solar radiation (~30% degradation efficiency) [100].

Liu et al. have reported for the first time a hierarchical-nanostructured coating comprising of aluminum zinc oxide (AZO), deposited on a glass substrate through atmospheric plasma spraying. The coatings were of 60 μm thickness and porosity of 24%. The E_g value of the coating sample was 3.24 eV. Related to the photodegradation efficiency of these coatings a decrease of 36% in methylene blue concentration has been observed after 72 hours of UV irradiation [101].

Recently, a new technique has been developed by Sulzer Metco AG (Switzerland), which combines the physical vapor deposition (PVD) method with the low-pressure plasma spraying (LPPS) or vacuum plasma spraying (VPS) variant of thermal spraying. The advantage of this technique is that it can deposit coatings out of the vapor phase. This process uses a high energy plasma gun operated at a reduced work pressure of 0.1 kPa (1 mbar) which accelerates and projects the vaporized feedstock material that impacts the cooled substrate, thus resulting unique coating microstructures [102]. Up to date it has been used only for obtaining ceramic thermal barriers and hard coatings, but its extension to the obtaining of photocatalytic surfaces would be very promising [103].

2.4. Cold spraying

This variant of thermal spraying has been implemented already for obtaining corrosion- and

wear-resistant coatings or for electromagnetic interference shielding [18,104,105]. In cold spraying (CS) (also named cold gas spraying), the feedstock particles are accelerated to supersonic velocities, like in the HVOF variant, but in CS they are being maintained at temperatures significantly lower than their melting point for their entire time of flight. Inert carrier gasses can be used to minimize oxidation (Figure 6). Depending on the process parameters, the impact velocity with the substrate is in the 200–1500 m/s range. Interparticle or particle/substrate bonding is facilitated mainly by plastic deformation [106–109].

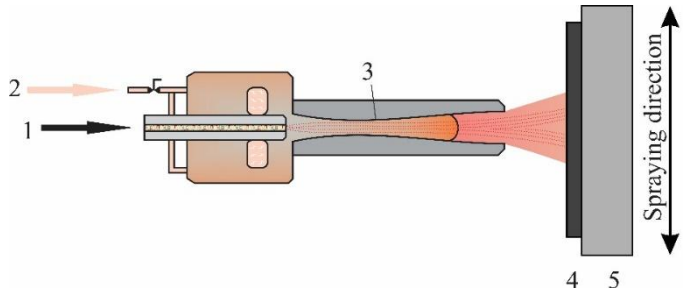

Figure 6. Principle of cold spraying. 1: filler material (powder) and carrier gas; 2: process gas; 3: Laval type nozzle; 4: thermal spray deposit; 5: base material [48].

Regarding photocatalytic coatings, most cold spraying applications resume to titania. Yang et al. have used TiO_2 anatase powders (10–45 μm) to obtain nanopatterned coatings on stainless steel by cold gas spraying, using nitrogen as a driving/carrier gas with an inlet pressure of 2.0 MPa and temperature of 300 °C. Higher anatase contents have been reported by comparing to the typical values obtained through plasma or HVOF spraying, owing to the lower deposition temperatures. The photocatalytic response of the coatings was evaluated against gaseous acetaldehyde under UV irradiation. Almost complete removal of this model pollutant as achieved after 30 minutes of irradiation [110].

Yamada et al. have concluded that cold spraying is an ideal process for fabricating anatase-rich TiO_2 photocatalyst coating. The anatase structure could be preserved by carefully controlling the spraying parameters, mainly the processing gas temperatures (200–400 °C), which are below the anatase to rutile transition temperature. The nature of the gas (nitrogen or helium) does not seem to have a significant influence on the performance of the coatings [111]. Cold spray was employed by Yang et al. for obtaining TiO_2 photocatalytic films with thickness of ~15 μm. The photocatalytic performance was examined through acetaldehyde degradation under ultraviolet illumination. Results showed that no phase and particle size changes occurred to TiO_2 during deposition, and the coating was efficient towards degradation of acetaldehyde [112]. The low deposition temperatures of the cold gas spraying process allow for deposition on polymer or glass substrates, otherwise unfeasible by traditional flame and plasma spraying methods [113]. Robotti et al. have obtained 200–400 μm-thick nanopatterned titania coatings on polymer substrates with good photodegradation yield against NO_x (~20–80%) under UV irradiation [114]. Composite coatings with various surface chemistry have been obtained by Park et al. starting from ATO (Sb_2O_5:SnO_2, 15:85 wt%, 13–22 nm) and titania (15 nm) nanopowders using FTO glass as substrate. The complete photocatalytic decolorization of methylene blue in an aqueous solution under UV light irradiation has been achieved after 6 hours [115].

A relatively new variant approach of this thermal spraying method is represented by vacuum cold spraying. Through this technique an optimum balance can be achieved between a high photocatalytic activity (fine structure and large surface area) and a good adhesion between coating and substrate surface [116]. For example, Yao et al. have demonstrated by molecular dynamic simulation that nano-scale feedstock powders are subjected to an increased localized plastic deformation during collision at low velocities, while at high velocities the intensive deformation promotes the nanoparticles adhesion rather than rebounding off [117].

Yao et al. prepared a composite nano-TiO_2/polyethyleneglycol (PEG) powder as feedstock material for vacuum cold spraying and the photocatalytic activity of the coatings was assessed through photodegradation of phenol in water. Results showed that post-deposition annealing of the coating between 450 and 500 ℃ yielded both higher activity and increased adhesion to the substrate. The TiO_2 coating, resulting from the composite powder/PEG feedstock presented much higher activity than that deposited with the primary nanopowders, which can be attributed to its high porosity, which facilitates the contact of the reactant with the photocatalyst phases [118].

3. Conclusion

The mechanisms underlying the photocatalytic response of thermal sprayed coatings reside in both the surface chemistry of the feedstock material or the in-situ generated material (i.e., its optical band gap) and the specific surface area of the coating. The latter is mainly influenced by the roughness and nanopatterning of the surface (obtaining of nano-aggregates). Thermal spraying offers the means to fine tune both the chemical composition of the coating (through choosing the appropriate feedstock material, spraying distance, gasses involved in combustion/transport, etc.) as well as the roughness and the degree of clustering of the aggregates on the surface of the material.

Most of the research involving thermal spraying applied to photocatalytic coatings achievement deal with TiO_2 powders, powder suspensions or organic precursors which can generate the titania in-situ (in the flame or plasma). These coatings are mainly active in the UV-part of the electromagnetic radiation domain. Composite coatings bearing titania or doped titania can also be obtained with the plasma and HVOF spraying techniques, which present moderate photocatalytic activity in the visible domain. The second most frequent system employed in thermal spraying is based on ZnO, which possesses a lower band gap than TiO_2 and can harvest visible light more efficiently.

High velocity oxy-fuel spraying and cold spraying have been generally found to be up to 25–35% more efficient in the photodegradation of organic compounds compared with flame spraying or plasma spraying. For the latter techniques, polymorph structural conversions affect the photocatalytic yield, with unwanted material oxidation, substrate overheating and delamination from the substrate. Flame spraying, with its suspension flame spraying technological variant is a relatively simple method and the operational cost is significantly less than the other techniques, needing a careful choosing of the feedstock material and operational parameters.

Acknowledgments

We would like to thank the structural funds project PRO-DD (POS-CCE, O.2.2.1, ID 123, SMIS 2637, ctr. No 11/2009) for partly providing the means for accessing the international

research-indexing databases used in this work.

Conflict of interest

The authors declare no conflict of interest.

References

1. Martin PM (2010) *Handbook of Deposition Technologies for Films and Coatings: Science, Applications and Technology*, 3 Eds., Elsevier.
2. Ganesh VA, Raut HK, Nair AS, et al. (2011) A review on self-cleaning coatings. *J Mater Chem* 21: 16304–16322.
3. Fenker M, Balzer M, Kappl H (2014) Corrosion protection with hard coatings on steel: Past approaches and current research efforts. *Surf Coat Tech* 257: 182–205.
4. Grun R (1995) Combination of different plasma-assisted processes with pulsed d.c.: cleaning, nitriding and hardcoatings. *Surf Coat Tech* 74–75: 598–603.
5. Montemor MF (2014) Functional and smart coatings for corrosion protection: A review of recent advances. *Surf Coat Tech* 258: 17–37.
6. Kapridaki C, Pinho L, Mosquera MJ, et al. (2014) Producing photoactive, transparent and hydrophobic SiO_2-crystalline TiO_2 nanocomposites at ambient conditions with application as self-cleaning coatings. *Appl Catal B-Environ* 156: 416–427.
7. Nazeer AA, Madkour M (2018) Potential use of smart coatings for corrosion protection of metals and alloys: A review. *J Mol Liq* 253: 11–22.
8. Jansen JC, Koegler JH, van Bekkum H, et al. (1998) Zeolitic coatings and their potential use in catalysis. *Micropor Mesopor Mat* 21: 213–226.
9. Lejars M, Margaillan A, Bressy C (2012) Fouling release coatings: A nontoxic alternative to biocidal antifouling coatings. *Chem Rev* 112: 4347–4390.
10. Tetault N, Gbaguidi-Haore H, Bertrand X, et al. (2012) Biocidal activity of metalloacid-coated surfaces against multidrug-resistant microorganisms. *Antimicrob Resist In* 1: 35.
11. Coombs A, Lindenmo M, Snell D, et al. (2001) Review of the types, properties, advantages, and latest developments in insulating coatings on nonoriented electrical steels. *IEEE T Magn* 37: 544–557.
12. Huang X (2009) High temperature radiation heat transfer performance of thermal barrier coatings with multiple layered structures. *J Eng Gas Turb Power* 131: 011301.
13. Cheruvu NS, Wei R, Gandy DW (2010) Influence of thermal exposure on the stability of metastable microstructures of sputter deposited nanocrystalline 304 and 310 stainless steel coatings. *Surf Coat Tech* 205: 1211–1219.
14. Huang XX, Sun SC, Lu SD, et al. (2018) Synthesis and characterization of oxidation-resistant TiB_2 coating on molybdenum substrate by chemical vapor deposition. *Mater Lett* 228: 53–56.
15. Pascu A, Stanciu EM, Roata IC, et al. (2017) Influence of the Laser Cladding. Parameters and Solar Heat Treatment on the Properties of Biocompatible Inconel 718 Coatings. *Rev Rom Mater* 47: 157–165.
16. Stanciu EM, Pascu A, Tierean MH, et al. (2016) Dual Coating Laser Cladding of NiCrBSi and Inconel 718. *Mater Manuf Process* 31: 1556–1564.

17. Sudagar J, Lian JS, Sha W (2013) Electroless nickel, alloy, composite and nano coatings—A critical review. *J Alloy Compd* 571: 183–204.
18. Assadi H, Kreye H, Gartner F, et al. (2016) Cold spraying—A materials perspective. *Acta Mater* 116: 382–407.
19. Sivakumar G, Banerjee S, Raja VS, et al. (2018) Hot corrosion behavior of plasma sprayed powder-solution precursor hybrid thermal barrier coatings. *Surf Coat Tech* 349: 452–461.
20. Szymanski K, Hernas A, Moskal G, et al. (2015) Thermally sprayed coatings resistant to erosion and corrosion for power plant boilers—A review. *Surf Coat Tech* 268: 153–164.
21. Roata IC, Pascu A, Croitoru C, et al. (2017) Thermal Spraying of CuAlFe Powder on Cu_5Sn Alloy. *IOP Conf Ser Mater Sci Eng* 209: 012042.
22. Vaßen R, Jarligo MO, Steinke T, et al. (2010) Overview on advanced thermal barrier coatings. *Surf Coat Tech* 205: 938–942.
23. Karthikayan S, Ganesan S, Vasanthakumar P, et al. (2017) Innovative Research Trends in the Application of Thermal Barrier Metal Coating in Internal Combustion Engines. *Mater Today Proc* 4: 9004–9012.
24. Kosevic M, Stopic S, Cvetkovic V, et al. (2019) Mixed RuO_2/TiO_2 uniform microspheres synthesized by low-temperature ultrasonic spray pyrolysis and their advanced electrochemical performances. *Appl Surf Sci* 464: 1–9.
25. Brupbacher MC, Zhang DJ, Buchta WM, et al. (2018) Experimental characterization and physics-based modeling of the temperature-dependent diffuse reflectance of plasma-sprayed $Nd_2Zr_2O_7$ in the near to short-wave infrared. *Appl Optics* 57: 7782–7792.
26. Jing MX, Li J, Liu KG (2018) Research progress in photolectric materials of $CuFeS_2$. *IOP Conf Ser Earth Environ Sci* 128: 012087.
27. Heimann RB (2006) Thermal spraying of biomaterials. *Surf Coat Tech* 201: 2012–2019.
28. Marcano D, Mauer G, Vaßen R, et al. (2017) Manufacturing of high performance solid oxide fuel cells (SOFCs) with atmospheric plasma spraying (APS) and plasma spray-physical vapor deposition (PS-PVD). *Surf Coat Tech* 318: 170–177.
29. Fauchais P, Montavon G, Bertrand G (2010) From Powders to Thermally Sprayed Coatings. *J Therm Spray Techn* 19: 56–80.
30. Roata IC, Croitoru C, Pascu A, et al. (2018) Photocatalytic performance of copper-based coatings deposited by thermal spraying. *J Mater Sci-Mater El* 29: 11345–11357.
31. Feitosa FRP, Gomes RM, Silva MMR, et al. (2018) Effect of oxygen/fuel ratio on the microstructure and properties of HVOF-sprayed $Al_{59}Cu_{25.5}Fe_{12.5}B_3$ quasicrystalline coatings. *Surf Coat Tech* 353: 171–178.
32. Vardelle A, Moreau C, Themelis NJ, et al. (2015) A Perspective on Plasma Spray Technology. *Plasma Chem Plasma P* 35: 491–509.
33. Fauchais P, Vardelle A, Dussoubs B (2001) Quo vadis thermal spraying? *J Therm Spray Techn* 10: 44–66.
34. Byrne JA, Dunlop PSM, Hamilton JWJ, et al. (2015) A Review of Heterogeneous Photocatalysis for Water and Surface Disinfection. *Molecules* 20: 5574–5615.
35. Lazar MA, Tadvani JK, Tung WS, et al. (2010) Nanostructured Thin Films as Functional Coatings. *IOP Conf Ser Mater Sci Eng* 12: 012017.

36. Nikkanen JP, Huttunen-Saarivirta E, Salminen T, et al. (2015) Enhanced photoactive and photoelectrochemical properties of TiO_2 sol-gel coated steel by the application of SiO_2 intermediate layer. *Appl Catal B-Environ* 174: 533–543.
37. Guglielmi M (1997) Sol-Gel Coatings on Metals. *J Sol-Gel Sci Techn* 8: 443–449.
38. Darthout E, Laduye G, Gitzhofer F (2016) Processing Parameter Effects and Thermal Properties of $Y_2Si_2O_7$ Nanostructured Environmental Barrier Coatings Synthesized by Solution Precursor Induction Plasma Spraying. *J Therm Spray Techn* 25: 1264–1279.
39. Matejicek J, Chraska P, Linke J (2007) Thermal spray coatings for fusion applications—Review. *J Therm Spray Techn* 16: 64–83.
40. Pawlowski L (2009) Suspension and solution thermal spray coatings. *Surf Coat Tech* 203: 2807–2829.
41. Fauchais P, Montavon G, Lima RS, et al. (2011) Engineering a new class of thermal spray nano-based microstructures from agglomerated nanostructured particles, suspensions and solutions: An invited review. *J Phys D-Appl Phys* 44: 093001.
42. Gonzalez R, Ashrafizadeh H, Lopera A, et al. (2016) A Review of Thermal Spray Metallization of Polymer-Based Structures. *J Therm Spray Techn* 25: 897–919.
43. Kliemann JO, Gutzmann H, Gartner F, et al. (2011) Formation of Cold-Sprayed Ceramic Titanium Dioxide Layers on Metal Surfaces. *J Therm Spray Techn* 20: 292–298.
44. Chen X, Mao SS (2007) Titanium dioxide nanomaterials: Synthesis, properties, modifications, and applications. *Chem Rev* 107: 2891–2959.
45. Tomaszek R, Pawlowski L, Gengembre L, et al. (2006) Microstructural characterization of plasma sprayed TiO_2 functional coating with gradient of crystal grain size. *Surf Coat Tech* 201: 45–56.
46. Bozorgtabar M, Rahimipour M, Salehi M (2009) Effect of thermal spray processes on anatase–rutile phase transformation in nano-structured TiO_2 photo-catalyst coatings. *Surf Eng* 26: 422–427.
47. Yao HL, Hu XZ, Bai XB, et al. (2018) Comparative study of HA/TiO_2 and HA/ZrO_2 composite coatings deposited by high-velocity suspension flame spray (HVSFS). *Surf Coat Tech* 351: 177–187.
48. Roata IC (2018) *Applications of thermal spray technologies*, Brasov: LUX LIBRIS Publishing House.
49. Torres B, Campo M, Lieblich M, et al. (2013) Oxy-acetylene flame thermal sprayed coatings of aluminium matrix composites reinforced with $MoSi_2$ intermetallic particles. *Surf Coat Tech* 236: 274–283.
50. Yang GJ, Li CJ, Han F, et al. (2004) Effects of annealing treatment on microstructure and photocatalytic performance of nanostructured TiO_2 coatings through flame spraying with liquid feedstocks. *J Vac Sci Technol B* 22: 2364–2368.
51. Roata IC, Iovanas R, Pascu A (2013) Influence of the Metallizing Distance Variation and of the Electric Field Voltage on the Ohmic Resistance of the Layers Deposited by Thermal Spraying. *Metal Int* 18: 73–76.
52. Roata IC, Iovanas R, Iovanas DM (2011) The influence of powders cladded with electric charges upon the adherence of the layers that are deposited by metallization. *Metal Int* 16: 161–165.

53. Krieg P, Killinger A, Gadow R, et al. (2017) High velocity suspension flame spraying (HVSFS) of metal doped bioceramic coatings. *Bioact Mater* 2: 162–169.
54. Bolelli G, Cannillo V, Gadow R, et al. (2009) Properties of High Velocity Suspension Flame Sprayed (HVSFS) TiO_2 coatings. *Surf Coat Tech* 203: 1722–1732.
55. Boningari T, Inturi SNR, Suidan M, et al. (2018) Novel one-step synthesis of nitrogen-doped TiO_2 by flame aerosol technique for visible-light photocatalysis: Effect of synthesis parameters and secondary nitrogen (N) source. *Chem Eng J* 350: 324–334.
56. Bemer D, Regnier R, Subra I, et al. (2010) Ultrafine particles emitted by flame and electric arc guns for thermal spraying of metals. *Ann Occup Hyg* 54: 607–614.
57. Yang GJ, Li CJ, Wang YY (2005) Phase formation of nano-TiO_2 particles during flame spraying with liquid feedstock. *J Therm Spray Techn* 14: 480–486.
58. Yang GJ, Li CJ, Huang XC, et al. (2007) Influence of silver doping on photocatalytic activity of liquid-flame-sprayed-nanostructured TiO_2 coating. *J Therm Spray Techn* 16: 881–885.
59. Yang GJ, Li CJ, Li CX, et al. (2006) Effect of Cu^{2+} doping on photocatalytic performance of liquid flame sprayed TiO_2 coatings. *J Therm Spray Techn* 15: 582–586.
60. Ctibor P, Stengl V, Zahalka F, et al. (2011) Microstructure and performance of titanium oxide coatings sprayed by oxygen-acetylene flame. *Photoch Photobio Sci* 10: 403–407.
61. Kavitha R, Meghani S, Jayaram V (2007) Synthesis of titania films by combustion flame spray pyrolysis technique and its characterization for photocatalysis. *Mater Sci Eng B-Adv* 139: 134–140.
62. Navidpour AH, Salehi M, Amirnasr M, et al. (2015) Photocatalytic Iron Oxide Coatings Produced by Thermal Spraying Process. *J Therm Spray Techn* 24: 1487–1497.
63. Huang J, Gong YF, Liu Y, et al. (2017) Developing titania-hydroxyapatite-reduced graphene oxide nanocomposite coatings by liquid flame spray deposition for photocatalytic applications. *J Eur Ceram Soc* 37: 3705–3711.
64. Sassatelli P, Bolelli G, Gualtieri ML, et al. (2018) Properties of HVOF-sprayed Stellite-6 coatings. *Surf Coat Tech* 338: 45–62.
65. Li MH, Christofides PD (2009) Modeling and Control of High-Velocity Oxygen-Fuel (HVOF) Thermal Spray: A Tutorial Review. *J Therm Spray Techn* 18: 753–768.
66. Li CJ, Yang GJ (2013) Relationships between feedstock structure, particle parameter, coating deposition, microstructure and properties for thermally sprayed conventional and nanostructured WC-Co. *Int J Refract Met H* 39: 2–17.
67. Yang GJ, Li CJ, Wang YY, et al. (2007) Dominant microstructural feature over photocatalytic activity of high velocity oxy-fuel sprayed TiO_2 coating. *Surf Coat Tech* 202: 63–68.
68. Hanaor DAH, Sorrell CC (2011) Review of the anatase to rutile phase transformation. *J Mater Sci* 46: 855–874.
69. Toma FL, Berger LM, Shakhverdova I, et al. (2014) Parameters Influencing the Photocatalytic Activity of Suspension-Sprayed TiO_2 Coatings. *J Therm Spray Techn* 23: 1037–1053.
70. Toma FL, Berger LM, Jacquet D, et al. (2009) Comparative study on the photocatalytic behaviour of titanium oxide thermal sprayed coatings from powders and suspensions. *Surf Coat Tech* 203: 2150–2156.
71. Toma FL, Sokolov D, Bertrand G, et al. (2006) Comparison of the photocatalytic behavior of TiO_2 coatings elaborated by different thermal spraying processes. *J Therm Spray Techn* 15: 576–581.

72. Colmenares-Angulo J, Zhao S, Young C, et al. (2009) The effects of thermal spray technique and post-deposition treatment on the photocatalytic activity of TiO_2 coatings. *Surf Coat Tech* 204: 423–427.
73. Yang GJ, Li CJ, Wang YY, et al. (2008) Origin of preferential orientation of rutile phase in thermally sprayed TiO_2 coatings. *Mater Lett* 62: 1670–1672.
74. Yang GJ, Li CJ, Han F, et al. (2004) Microstructure and photocatalytic performance of high velocity oxy-fuel sprayed TiO_2 coatings. *Thin Solid Films* 466: 81–85.
75. Toma FL, Bertrand G, Klein D, et al. (2008) Development of photocatalytic active TiO_2 surfaces by thermal spraying of nanopowders. *J Nanomater* 2008: 58.
76. Ctibor P, Stengl V, Pala Z (2013) Structural and photocatalytic characteristics of TiO_2 coatings produced by various thermal spray techniques. *J Adv Ceram* 2: 218–226.
77. Gardon M, Guilemany JM (2014) Milestones in Functional Titanium Dioxide Thermal Spray Coatings: A Review. *J Therm Spray Techn* 23: 577–595.
78. Bozorgtabar M, Rahimipour M, Salehi M (2010) Novel photocatalytic TiO_2 coatings produced by HVOF thermal spraying process. *Mater Lett* 64: 1173–1175.
79. Pala Z, Shaw E, Murray JW, et al. (2017) Suspension high velocity oxy-fuel spraying of TiO_2: A quantitative approach to phase composition. *J Eur Ceram Soc* 37: 801–810.
80. Yu Z, Moussa H, Chouchene B, et al. (2018) One-step synthesis and deposition of $ZnFe_2O_4$ related composite films via SPPS route for photodegradation application. *Nanotechnology* 30: 045707.
81. Liu MJ, Zhang M, Zhang Q, et al. (2018) Gaseous material capacity of open plasma jet in plasma spray-physical vapor deposition process. *Appl Surf Sci* 428: 877–884.
82. Yao JT, Ren JQ, Huo HB, et al. (2014) Deposition behavior of semi-molten spray particles during flame spraying of porous metal alloy. *J Therm Spray Techn* 23: 991–999.
83. Toma FL, Bertrand G, Chwa SO, et al. (2006) Comparative study on the photocatalytic decomposition of nitrogen oxides using TiO_2 coatings prepared by conventional plasma spraying and suspension plasma spraying. *Surf Coat Tech* 200: 5855–5862.
84. Dosta S, Robotti M, Garcia-Segura S, et al. (2016) Influence of atmospheric plasma spraying on the solar photoelectro-catalytic properties of TiO_2 coatings. *Appl Catal B-Environ* 189: 151–159.
85. Vu P, Otto N, Vogel A, et al. (2018) Efficiently quantifying the anatase content and investigating its effect on the photocatalytic activity of titania coatings by suspension plasma spraying. *Surf Coat Tech*.
86. Solonenko OP, Ando Y, Nishiyama H, et al. (2018) Synthesis of thick photocatalytic titania surface layers by solution plasma spraying and subsequent treatment by pulsed laminar plasma jet. *Surf Coat Tech* 333: 39–51.
87. Wang CL, Hwang WS, Chu HL, et al. (2016) Kinetics of anatase transition to rutile TiO_2 from titanium dioxide precursor powders synthesized by a sol-gel process. *Ceram Int* 42: 13136–13143.
88. Ctibor P, Seshadri RC, Henych J, et al. (2016) Photocatalytic and electrochemical properties of single- and multi-layer sub-stoichiometric titanium oxide coatings prepared by atmospheric plasma spraying. *J Adv Ceram* 5: 126–136.
89. Daram P, Banjongprasert C, Thongsuwan W, et al. (2016) Microstructure and photocatalytic activities of thermal sprayed titanium dioxide/carbon nanotubes composite coatings. *Surf Coat Tech* 306: 290–294.

90. Zhai MJ, Liu Y, Huang J, et al. (2019) Efficient suspension plasma spray fabrication of black titanium dioxide coatings with visible light absorption performances. *Ceram Int* 45: 930–935.
91. Ctibor P, Pala Z, Stengl V, et al. (2014) Photocatalytic activity of visible-light-active iron-doped coatings prepared by plasma spraying. *Ceram Int* 40: 2365–2372.
92. Yu ZX, Moussa H, Ma YZ, et al. (2019) Oxygen-defective ZnO films with various nanostructures prepared via a rapid one-step process and corresponding photocatalytic degradation applications. *J Colloid Interf Sci* 534: 637–648.
93. Yu ZX, Moussa H, Liu MM, et al. (2018) Solution precursor plasma spray process as an alternative rapid one-step route for the development of hierarchical ZnO films for improved photocatalytic degradation. *Ceram Int* 44: 2085–2092.
94. Navidpour AH, Kalantari Y, Salehi M, et al. (2017) Plasma-Sprayed Photocatalytic Zinc Oxide Coatings. *J Therm Spray Techn* 26: 717–727.
95. Chen D, Jordan EH, Gell M (2008) Porous TiO_2 coating using the solution precursor plasma spray process. *Surf Coat Tech* 202: 6113–6119.
96. Zeng Y, Liu JT, Wu W, et al. (2005) Photocatalytic performance of plasma sprayed TiO_2–$ZnFe_2O_4$ coatings. *Surf Coat Tech* 200: 2398–2402.
97. Liu JT, Zeng Y, Zhao XB, et al. (2005) Photocatalytic performance of plasma sprayed TiO_2–$ZnFe_2O_4$ coatings. *Mater Sci Forum* 486–487: 69–72.
98. Zeng Y, Wu W, Lee S, et al. (2007) Photocatalytic performance of plasma sprayed Pt-modified TiO2 coatings under visible light irradiation. *Catal Commun* 8: 906–912.
99. Ye FX, Tsumura T, Nakata K, et al. (2008) Dependence of photocatalytic activity on the compositions and photo-absorption of functional TiO_2–Fe_3O_4 coatings deposited by plasma spray. *Mater Sci Eng B-Adv* 148: 154–161.
100. Dom R, Sivakumar G, Hebalkar NY, et al. (2012) Deposition of nanostructured photocatalytic zinc ferrite films using solution precursor plasma spraying. *Mater Res Bull* 47: 562–570.
101. Liu WH, Shieu FS, Hsiao WT (2017) AZO photocatalytic coating deposited by plasma thermal spraying with shell-type feedstock powder. *J Eur Ceram Soc* 37: 2857–2869.
102. Von Niessen K, Gindrat M (2011) Plasma spray-PVD: A new thermal spray process to deposit out of the vapor phase. *J Therm Spray Techn* 20: 736–743.
103. Gao L, Guo H, Wei L, et al. (2015) Microstructure and mechanical properties of yttria stabilized zirconia coatings prepared by plasma spray physical vapor deposition. *Ceram Int* 41: 8305–8311.
104. Lee JG, Kim DY, Lee JH, et al. (2016) Scalable Binder-Free Supersonic Cold Spraying of Nanotextured Cupric Oxide (CuO) Films as Efficient Photocathodes. *ACS Appl Mater Inter* 8: 15406–15414.
105. Schmidt T, Gartner F, Assadi H, et al. (2006) Development of a generalized parameter window for cold spray deposition. *Acta Mater* 54: 729–742.
106. Herrmann-Geppert I, Bogdanoff P, Emmler T, et al. (2016) Cold gas spraying—A promising technique for photoelectrodes: The example TiO_2. *Catal Today* 260: 140–147.
107. Yang GJ, Liao KX, Li CJ, et al. (2012) Formation of Pore Structure and Its Influence on the Mass Transport Property of Vacuum Cold Sprayed TiO_2 Coatings Using Strengthened Nanostructured Powder. *J Therm Spray Techn* 21: 505–513.

108. Li CJ, Yang GJ, Huang XC, et al. (2004) Formation of TiO_2 photocatalyst through cold spraying. *International Thermal Spray Conference 2004: Advances in Technology and Application*, 315–319.
109. Li CJ, Li WY (2003) Deposition characteristics of titanium coating in cold spraying. *Surf Coat Tech* 167: 278–283.
110. Fan SQ, Li CJ, Yang GJ, et al. (2008) Room-temperature deposition of nano-TiO_2 coating by vacuum cold spraying using $TiCl_4$-agglomerated nano-TiO_2 powder for flexible dye-sensitized solar cell. *Key Eng Mater* 373–374: 742–745.
111. Yamada M, Isago H, Nakano H, et al. (2010) Cold spraying of TiO_2 photocatalyst coating with nitrogen process gas. *J Therm Spray Techn* 19: 1218–1223.
112. Yang GJ, Li CJ, Han F, et al. (2008) Low temperature deposition and characterization of TiO_2 photocatalytic film through cold spray. *Appl Surf Sci* 254: 3979–3982.
113. Zhou XL, Chen AF, Liu JC, et al. (2011) Preparation of metallic coatings on polymer matrix composites by cold spray. *Surf Coat Tech* 206: 132–136.
114. Robotti M, Dosta S, Fernandez-Rodriguez C, et al. (2016) Photocatalytic abatement of NOx by C-TiO_2/polymer composite coatings obtained by low pressure cold gas spraying. *Appl Surf Sci* 362: 274–280.
115. Park Y, Kim H, Pawar RC, et al. (2018) Photocatalytic evaluation of ATO/TiO_2 heterojunction films fabricated by a nanoparticle deposition system. *Mater Chem Phys* 203: 118–124.
116. Yao HL, Hu XZ, Yang GJ (2017) Effect of Particle Size and Impact Velocity on Collision Behaviors Between Nano-Scale TiN Particles: MD Simulation. *J Nanosci Nanotechno* 18: 4121–4126.
117. Yao HL, Yang GJ, Li CJ (2017) MD Simulation on Collision Behavior Between Nano-Scale TiO_2 Particles During Vacuum Cold Spraying. *J Nanosci Nanotechno* 18: 2657–2664.
118. Yang GJ, Li CJ, Fan SQ, et al. (2007) Influence of annealing on photocatalytic performance and adhesion of vacuum cold-sprayed nanostructured TiO_2 coating. *J Therm Spray Techn* 16: 873–880.

AIMS Press